
PERGAMON

Corrosion Science 45 (2003) 957–966

CORROSION SCIENCE

www.elsevier.com/locate/corsci

Effect of MnS powder addition and sintering temperature on the corrosion resistance of sintered 303LSC stainless steels

Wen-Fung Wang *

Department of Mechanical Engineering, Southern Taiwan University of Technology, Tainan 700, Taiwan

Received 17 December 2001; accepted 11 September 2002

Abstract

As the sintered parts are to be machined after sintering the MnS powder is usually added to improve the machinability. Effect of the MnS powder content on the corrosion resistance of the sintered 303LSC alloys was investigated. Experimental results show that the addition of MnS powder decreases the green density of the 303LSC compacts. The sintered density of the admixed powder compacts slightly increase with increasing MnS content. The weight loss rate of the sintered specimens being immersed in the 10% $FeCl_3$ corrosion test solution increases with increasing MnS content. The corrosion resistance is improved with increasing sintering temperature. The metallographic evolution of the corroded surface was studied.

Keywords: MnS addition; Sintered 303LSC stainless steel; Corrosion resistance

1. Introduction

Most of the sintered structural parts have near-net shape, the secondary operation is generally not necessary. But the holes perpendicular to the compacting direction, thread and undercut can only be finished by machining. Recently the secondary operation like machining is fast becoming an essential step in the production of a large variety of powder metallurgy components. It is estimated that about 30% of all sintered automotive parts required some machining operation. However, the machinability of the sintered structural parts is inherently inferior to that of the conventional

* Fax: +886-6-268-5257.
E-mail address: abstotal@ms17.hinet.net (W.-F. Wang).

0010-938X/03/$ - see front matter
PII: S0010-938X(02)00181-6

cast-wrought materials. The pores in the sintered parts result in a non-continuous contact between the workpiece and the cutting edge of the tool, causing an interrupted cut and subsequent tool wear. Also, the pores contribute toward a reduced thermal conductivity, resulting in a slower dissipation of heat. This can induce high temperature at the tool–workpiece interface and cause a rapid tool failure.

The factors affecting the machinability of powder metallurgy materials include: material porosity, manufacturing process, alloy chemistry, machining variable, and the alloy microstructure [1]. Sintering practices can influence the pore structure, surface chemistry, and the microstructure of the sintered alloy. As an example, surface oxide and the presence of certain inclusions can degrade the machinability [2,3]. It is possible to improve the machinability of P/M parts by modifying their microstructure. Some works have been reported that the use of heat treatment cycles can modify the microstructure and influence their machinability [4,5]. However, the popular and convenient technique to improve the machinability involves the addition of machining aid.

Addition of various machining aids to improve the machinability of the ferrous P/M parts has been investigated by a number of authors [2–4,6–12]. Machining aids investigated include, MnS, Pb, Bi, Te, Se, and MoS_2 powders. These additives are either incorporated into the melt before powder production or mixed-in during the mixing stage. Manganese sulfide (MnS) powder is the most widely used and probably the most effective additive to improve the machinability of ferrous alloys. Addition of manganese sulfide powder has been reported to improve the machinability of various P/M alloys, including: carbon steels, copper steels, nickel steels, low-alloy steels, stainless steels, and soft magnetic steels [2,7,8,10–17]. During the machining operation, the malleable MnS particles deform easily and coat the tool surface. Thus, the presence of MnS on the tool surface helps to reduce the friction between the tool surface and the workpiece. This in turn results in reduced tool wear, lower machining temperature and longer tool life. Further, it was demonstrated that the addition of small quantities of MnS has minimal effect on the mechanical and physical properties of these alloys. However, these published works did not deal with the effect of MnS powder addition on the corrosion resistance of various sintered steels.

Most stainless steels available for powder metallurgy are copies of wrought alloys. While the wrought compositions have been optimized with respect to their fabrication schedules and corrosion resistance. Thus it is not surprising to see that sintered alloys often exhibit inferior corrosion resistance. The inferior corrosion properties are resulted from compound formation, precipitation, and reaction with the atmosphere during sintering, as well as a higher surface area due to porosity [18–28]. Vacuum sintering or using a pure hydrogen with a dew point below −40 °C can avoid reaction between the compacts and the sintering atmosphere. There is no chromium depletion through the formation of oxides and nitrides. Consequently the corrosion problem is partly reduced [29].

The corrosion resistance of the alloys containing two phases or more is always inferior to that of the simple solid solution. In addition to the inherent porosity, the introducing of MnS powder may further decrease the corrosion resistance of the sintered stainless steels. The present investigation was carried out to study the effect

of MnS powder addition on the compactability and sinterability of the 303LSC stainless steel powder. How the corrosion resistance of the sintered 303LSC alloys varied with the MnS content and the metallographic evolution of the eroded surface during the corrosive immersion test were studied. Interaction between the MnS particles and the 303LSC matrix during sintering was also examined.

2. Experimental

The 303LSC stainless steel powder used was water-atomized with a particle size of −100 mesh, its chemical composition is Cr 18.9 wt.%, Ni 12.8 wt.%, C 0.03 wt.%, Sn 0.8 wt.%, and Cu 2.0 wt.%. The matrix powder has been admixed with the compacting lubricant that is composed of 0.3 wt.% lithium stearate and 0.7 wt.% Acrawax. The particle size of the MnS powder is −325 mesh. The MnS powder was added with 0, 0.2, 0.4, 0.6, 0.8, 1.0 and 1.2 wt.%, respectively. After mixing, the mixed powder was consolidated into cylindrical compacts at a pressure of 490 MPa. The compacts were then sintered at 1100, 1150, 1200 and 1250 °C for 40 min in bottled hydrogen (with a dew point of −40 °C). The diameter, thickness and weight of the specimens before and after sintering were measured. The green density, dimensional change and sintered density were calculated to investigate the effect of MnS content on the compactability and sinterability of the 303LSC stainless steel powder.

Effect of the MnS powder addition on the corrosion resistance of sintered 303LSC stainless steels was studied by the immersion test. The sintered specimens were immersed in the 10% $FeCl_3$ solution for 24 h, then water-rinsed, dried, and the weight loss was measured. The erosion solution was slowly stirred. The lab was air-conditioned to keep the room temperature at 25 °C when the experiment was conducted. During immersion the rust did not accumulated on the specimen surface, but dissolved in the solution. The immersion test was carried out five times. The sum of weight loss was divided by five to obtain the weight loss rate (mg/cm^2 day). To study the metallographic evolution of the corroding surface the sintered specimens were ground, polishing and immersed in the $FeCl_3$ solution for some time interval, then washed, dried and examined with an optical microscope.

The sintered specimens were examined with a scanning electron microscope. Interaction between the MnS particles and the 303LSC matrix during sintering was investigated by the X-ray mapping. The intensity of the composition elements in both phases was measured by point counting. The acceleration voltage was 15 kV.

3. Experimental results and discussion

3.1. Effect of the MnS content on the compactability and sinterability of the 303LSC powder

Fig. 1 shows the variation of green and sintered densities with the MnS content and the sintering temperature. The green density decreases monotonously with

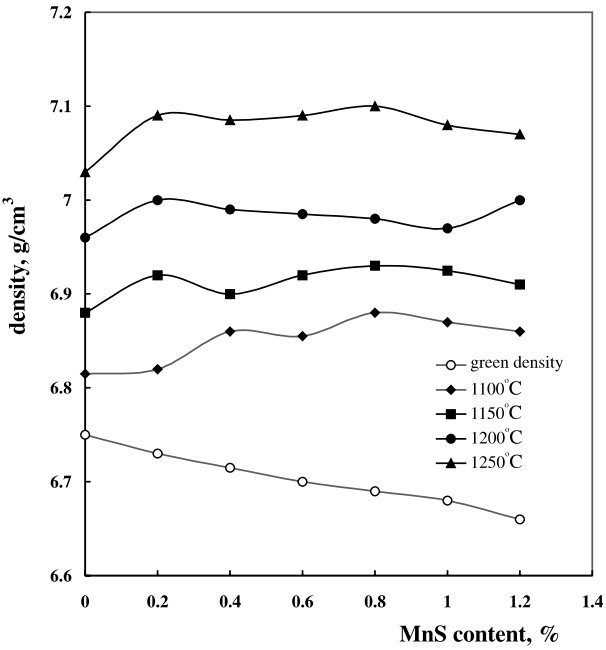

Fig. 1. Variation of the green and sintered densities with the MnS content and the sintering temperature.

increasing MnS content owing to the low specific gravity of the MnS powder. The sintered density increases with increasing temperature. Addition of the MnS powder does not degrade the sinterability of the 303LSC powder. The sintered density slightly increases with increasing MnS content for the group of specimens sintered at the same temperature. However, the difference in density is always less than 0.1 g/cm^3.

3.2. Effect of the MnS content and sintering temperature on the corrosion resistance of the sintered 303LSC stainless steels

After being immersed in the 10% $FeCl_3$ corrosion test solution for five days, the variation of the weight loss rate of sintered 303LSC stainless steels with the MnS content and the sintering temperature is shown in Fig. 2. The weight loss rate increases with increasing MnS content. The corrosion resistance of the sintered 303LSC stainless steels is reduced by the addition of the MnS powder. The contact area between the MnS particle and the 303LSC matrix is property-discontinuous, these two phases are pressed together by the mechanical force. As being immersed in the corrosive medium crevice corrosion is apt to initiate on the contact region. Therefore, adding more MnS powder provides more sites to induce the crevice corrosion.

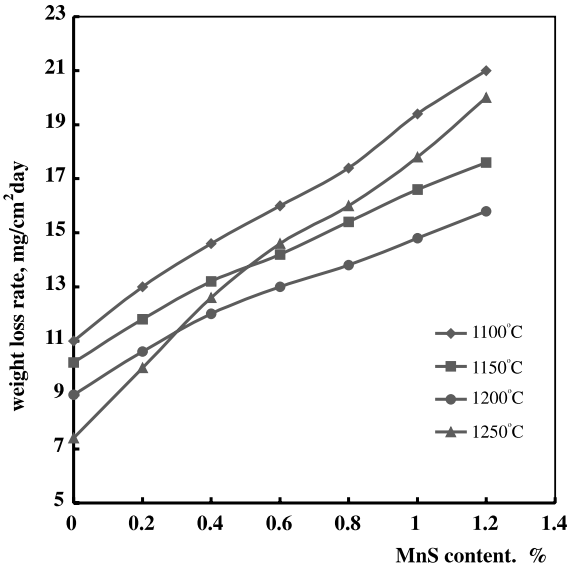

Fig. 2. Variation of weight loss rate with the MnS content and the sintering temperature after being immersed in the 10% $FeCl_3$ solution for 120 h.

The corrosion resistance of the sintered alloys is improved with increasing sintering temperature. As the sintering temperature raises from 1100 to 1150 °C, the weight loss rate is significantly reduced. Higher sintered density and lower volume content of the interconnected pores will be resulted as the compacts are sintered at higher temperature. The surface area exposed to the corrosive medium is effectively reduced. When the sintering temperature is further increased from 1150 to 1200 °C, the upgrading of the corrosion resistance slightly decreases. Being sintered at 1200 °C, most of the open interconnected pores may be closed in the initial stage of sintering, and during densification the further density increment is mainly resulted from variation of the morphology of the isolated pores, such as pore spheroidization. As a result, the corrosion resistance of the sintered alloys is no longer closely related with the sintered density.

For the alloys sintered at 1250 °C and containing the MnS powder more than 0.6 wt.%, the corrosion resistance is degraded markedly in spite of their high sintered density. The weight loss rate of specimens containing 0.6, 0.8, 1.0, and 1.2 wt.% MnS becomes higher than that of the alloys sintered at 1150 °C. Here, the sintered density is no longer the dominant factor affecting the corrosion resistance of the sintered stainless steels.

Fig. 3 is the X-ray map of chromium, iron and sulfur of the MnS-added 303LSC alloy sintered at 1250 °C. The dark area on the left-hand side of Fig. 3a is the MnS particle, and the right gray zone is the 303LSC matrix. Fig. 3b is the X-ray map of sulfur, there shows that some sulfur atoms migrated across the phase boundary and diffused into the 303LSC matrix. Fig. 3c is the X-ray map of chromium, it can be

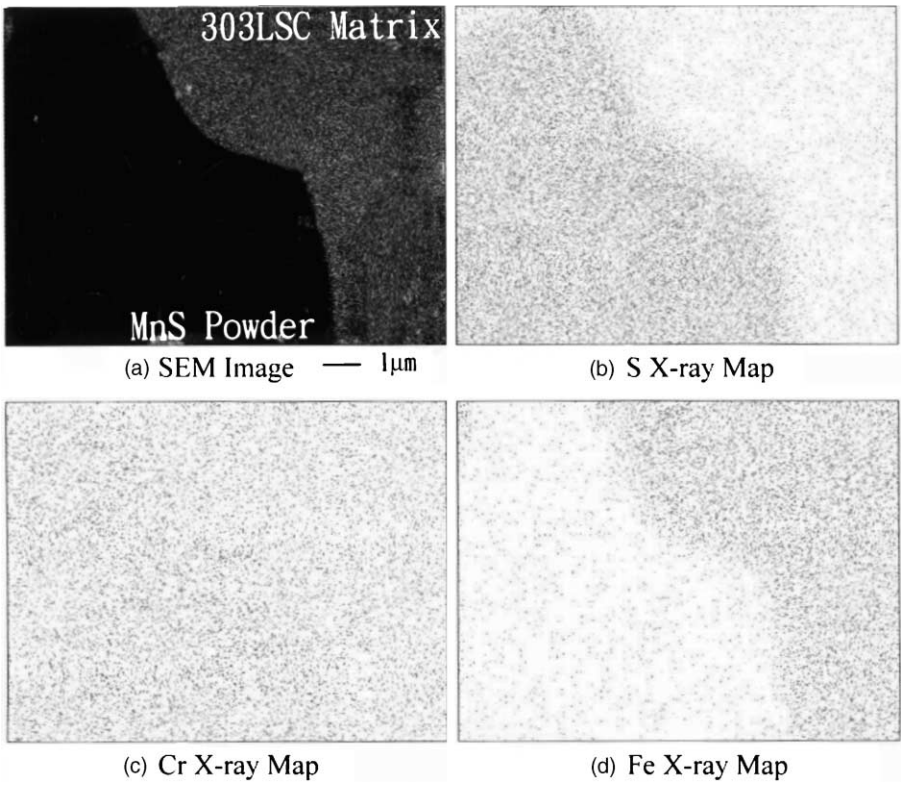

Fig. 3. SEM image and X-ray maps of 303LSC + 1.2% MnS, sintered at 1250 °C to a density of 7.1 g/cm^3.

seen that the Cr atoms fairly uniformly distributed in both phases. Upon carefully examining, it is found that the point intensity of chromium in the MnS region is a little higher than that in the 303LSC matrix. Fig. 3d shows the distribution of the Fe element, a few iron atoms diffused from the matrix into the MnS particle.

The results of X-ray mapping show that an intensive reaction occurred between the MnS particle and the alloy matrix during sintering at 1250 °C. This finding is in contrast with that of Madan's work [2] which stated that the MnS powder was stable at the sintering temperature and did not interact with the matrix material. The chromium atoms are more active and exhibit a higher diffusion rate in the MnS compound. Line scanning and point counting have also been performed on the specimen shown in Fig. 3a. The measured results of point counting indicate that the chemical composition of the MnS particle is S 35–36 wt.%, Mn 30–32 wt.%, Fe 2–4 wt.%, Ni 2–3 wt.%, and Cr 26–30 wt.%, and that of the 303LSC matrix within a distance of 6 μm from the phase boundary is S 1.5–2 wt.%, Mn 0.25–0.3 wt.%, Ni 12.5–13 wt.% and the Cr content decreases from the original 18.7–19 wt.% to a value of about 17 wt.%. A marked chromium-loss occurred in this area. Examining other three groups of specimens sintered below 1200 °C chromium enrichment in the MnS

particles has also been detected, however, the Cr-loss in the 303LSC matrix was not found. Therefore, a marked chromium diminution of the 303LSC matrix in the area neighboring the phase boundary may be the main reason that the corrosion resistance of the MnS-added 303LSC alloys sintered at 1250 °C degrades abnormally.

A similar situation has been found as the stainless steel powder compacts were sintered in the dissociated ammonia, the corrosion resistance of the sintered alloys was significantly reduced owing to the chromium decreasing. During sintering the nitrogen in the dissociated ammonia reacted with the chromium atoms to form the chromium nitride and caused chromium depletion at the surface of the sintered alloy [18,25,26,30].

3.3. Corrosion metallography

The specimens containing 1.2 wt.% MnS and respectively sintered at 1150 and 1250 °C were ground and polished, then immersed in the 10% $FeCl_3$ solution for some intervals. The washed and dried specimens were carefully observed with an optical microscope to study the metallographic evolution of the corroded surface. The effect of sintering temperature on the corrosion rate of these two groups of specimens was studied through the metallographic observation.

Fig. 4a is the MnS-containing 303LSC alloys before immersion. The particle shape of the MnS powder is irregular. The fine MnS particles uniformly distributed on the particle boundary of the 303LSC powder, and this might induce detrimental effect on the mechanical properties of the sintered alloy [15,16]. The large ones were squeezed into the intersection of the 303LSC particles and occupied the pore position during compacting. Fig. 4b is the 1150 °C-sintered specimen immersed in the $FeCl_3$ solution for 12 h. The contact area of the MnS particle and the 303LSC matrix was preferentially corroded and became a dark groove. This specimen includes two phases (MnS and 303LSC), therefore, its corrosion resistance is inferior to that of the simple 303LSC solid solution. These two phases possess different level of corrosion potential, the micro-anode and micro-cathode will be established. After establishing of these two poles, the galvanic corrosion will initiate at the contact area of these two phases.

In the solution including the chloride, the passive film of the stainless steels is unstable and the crevice corrosion is apt to occur. When there is fluid flowing or existing on the outside of contact area between the MnS particle and the 303LSC matrix, the fluid in this close contact crevice keeps stagnant. The chloride ions in the fluid will then induce corrosion. The stainless steel in the contact crevice is active and acts as the anode; the rest part outside is passive and acts as the cathode. Some potential difference exists between these two poles, and corrosion takes place at the anode. The anode reaction induces large amount of the metal cations that in turn attract the outside anions (especially the Cl^- ions) to move into the crevice and react with the cations to form the metal chloride. Hydrolysis of the metal chloride produces the hydrochloric acid that subsequently decreases the pH value of the solution in the crevice. Besides, decomposition of the hydrochloric acid gives more chloride ions to react with the metal cations. Increasing of the solution acidity results in

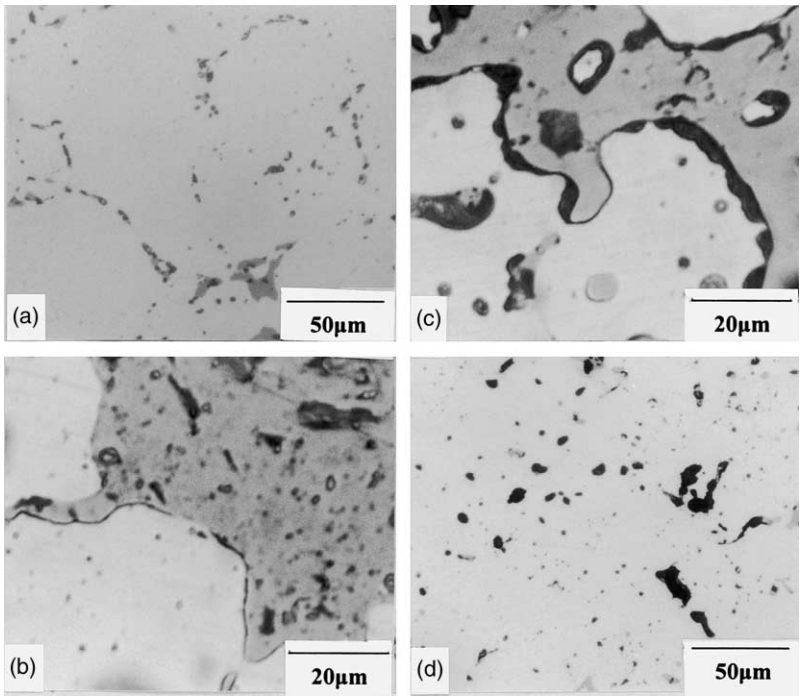

Fig. 4. Optical micrographs of sintered and eroded 303LSC + 1.2% MnS alloys (a) as-sintered at 1150 °C, (b) sintered at 1150 °C and eroded for 12 h, (c) sintered at 1250 °C and eroded for 12 h, (d) sintered at 1250 °C and eroded for 96 h.

collapse of the surface passive film and accelerates dissolving and corroding of the 303LSC alloys.

Fig. 4c is the 1250 °C-sintered specimen being immersion corroded for 12 h. The corroded groove induced on the phase boundary grew markedly. Carefully examining with the magnification of 1000 it was found that the corroded groove was wider at the top shallow part and deepened into the phase boundary in a step-downward manner. The upper part of the groove was in contact with the corrosive medium for a longer time and became wider for more mass being eroded away. Fig. 4d is the surface morphology of the 1250 °C-sintered specimen after being immersion eroded for 96 h. The small MnS particles disappear. As the crevice corrosion further extended inward along the contact area of the MnS particle and the 303LSC matrix, the small MnS particles would preferentially detach from the matrix, and black holes were left. The corroded holes then enlarged markedly.

4. Conclusion

1. The green density of the 303LSC compacts decreases with increasing MnS content. The sinterability of the 303LSC stainless steel powder did not degrade as

the MnS powder was added. The sintered densities slightly increase with increasing MnS content.

2. The corrosion resistance of the sintered 303LSC alloys decreases with increasing MnS content. The increasing of the sintering temperature improves the corrosion resistance of the sintered MnS-added 303LSC alloys, but the alloys containing the MnS higher than 0.6% and sintered at 1250 °C are exceptional.
3. Metallographic observation of the MnS-added specimens during the immersion test shows that the detrimental effect of MnS powder addition on the corrosion property of the sintered stainless steels results from the crevice corrosion that initiates on the contact region of the MnS particle and the 303LSC matrix. During further immersing the preferential detaching of small MnS particles and the ensued hole enlargement occur.

References

[1] J.S. Agapiou, M.F. DeVries, International Journal of Powder Metallurgy 24 (1) (1988) 47–57.
[2] D.S. Madan, Advances in Powder Metallurgy 13 (1991) 101–115.
[3] J.M. Cppus, C. Fournel, in: Modern Developments in Powder Metallurgy, vol. 13, Metal Powder Industries Federation, Princeton, NJ, 1981, pp. 137–142.
[4] R. Johnsson, in: Modern Developments in Powder Metallurgy, vol. 21, Metal Powder Industries Federation, Princeton, NJ, 1988, pp. 381–396.
[5] F.B. Fletcher, in: Modern Developments in Powder Metallurgy, vol. 10, Metal Powder Industries Federation, Princeton, NJ, 1977, pp. 453–466.
[6] P.W. Taubenblat, W.E. Smith, F.A. Bladt, in: Modern Developments in Powder Metallurgy, vol. 10, Metal Powder Industries Federation, Princeton, NJ, 1977, pp. 467–476.
[7] U. Engstron, Powder Metallurgy 26 (3) (1983) 137–144.
[8] Y. Trudel, C. Clilogu, S. Tremblay, in: Modern Developments in Powder Metallurgy, vol. 15, Metal Powder Industries Federation, Princeton, NJ, 1985, pp. 775–784.
[9] L.G. Roy, G. L'Esperance, P. Lambart, L.F. Pease, in: Progress in Powder Metallurgy, vol. 43, Metal Powder Industries Federation, Princeton, NJ, 1987, pp. 489–499.
[10] K.S. Chopra, D.S. Madan, in: Proceedings of the 1990 International Powder Metallurgy Conference, July 1990, Wembley, London, vol. 2, The Institute of Metals, 1990, pp. 61–70.
[11] K.S. Chopra, in: Progress in Powder Metallurgy, vol. 43, Metal Powder Industries Federation, Princeton, NJ, 1987, pp. 501–510.
[12] K.S. Chopra, in: Modern Developments in Powder Metallurgy, vol. 21, Metal Powder Industries Federation, Princeton, NJ, 1988, pp. 361–379.
[13] S. Suzuki, A. Hamazaki, I. Karasuno, M. Umino, in: Progress in Powder Metallurgy, vol. 43, Metal Powder Industries Federation, Princeton, NJ, 1987, pp. 511–520.
[14] D.S. Madan, in: Advances in Powder Metallurgy, vol. 13, Metal Powder Industries Federation, Princeton, NJ, 1992, pp. 53–79.
[15] Y.T. Chen, in: Advances in Powder Metallurgy, vol. 11, Metal Powder Industries Federation, Princeton, NJ, 1989, pp. 387–396.
[16] Y.T. Chen, in: Advances in Powder Metallurgy, vol. 12, Metal Powder Industries Federation, Princeton, NJ, 1990, pp. 13–28.
[17] A. Bhambri, L.F. Pease III, in: Modern Developments in Powder Metallurgy, vol. 18, Metal Powder Industries Federation, Princeton, NJ, 1988, pp. 155–182.
[18] H.S. Kalish, E.N. Mazza, Transaction TMS-AIME 203 (1955) 304–310.
[19] M.H. Tikkanen, A. Stosuy, P. Tunturi, Technical Bulletin, Hoeganaes Corp, Riverton, NJ, 1967.
[20] G. Jangg, O. Knotek, K. Faber, Planseeber, Pulvermet, 16, 1968, pp. 194–203.

[21] R.M.F. Jones, Progress in Powder Metallurgy 30 (1974) 25–50.
[22] M.Y. Nazmy, W. Karner, A.A. Al-Gwaiz, Journal of Metals 30 (6) (1978) 14–19.
[23] W. Karner, M.Y. Nazmy, A. Arfaj, in: Proceeding PM 78 SEMP, Concluding Volume, Stockholm, The European Symposium on Powder Metallurgy, 1978, pp. 212–239.
[24] D.H. Ro, E. Klar, in: H.H. Hausner, H.W. Antes, G.D. Smith (Eds.), Modern Development in Powder Metallurgy, vol. 18, Metal Powder Industries Federation, Princeton, NJ, 1981, pp. 247–287.
[25] H.S. Nayar, R.M. German, W.R. Johnson, Industrial Heating December (1981) 23–26.
[26] H.S. Nayar, R.M. German, W.R. Johnson, Progress in Powder Metallurgy 37 (1981) 255–265.
[27] M.A. Pao, E. Klar, in: Proceeding International Powder Metallurgy Conference, Florence, Italy, Associazione Italiana di Metallurgia, Milano, 1982, pp. 359–374.
[28] V.A. Douydenkov, I.D. Radomyselskii, S.G. Napara-Volgina, Soviet Powder Metallurgy and Ceramics 17 (1978) 371–379.
[29] R.L. Sands, G.F. Bidmead, D.A. Oliver, in: H.H. Hausner (Ed.), Modern Development in Powder Metallurgy, vol. 2, Plenum Press, New York, 1966, pp. 73–83.
[30] G. Lei, R.M. German, H.S. Nayar, Powder Metallurgy International 15 (2) (1983) 70–76.